

FIG. 3. Paramagnetic diffuse cross section $d\sigma/d\Omega_p$ in millibarns per Ce atom per steradian for $Ce_{0.8}Th_{0.2}$ versus T .

similar data for $x = 0.266$ and 0.29 . Since there is no evidence of a large conduction-electron compensating polarization, the small value of μ_{eff}^2 at 11 K is due to the small value of η , a small value of τ , and possibly crystal-field effects.

†Most of this work was performed while A. S. Edelstein had a summer faculty participation appointment at Oak Ridge National Laboratory and C. Tranchita had a summer appointment at Argonne National Laboratory.

*Research sponsored by the U. S. Energy Research and Development Administration under contract with Union Carbide Corporation.

¹R. A. Pollak, F. Holtzberg, J. L. Freeouf, and D. E. Eastman, *Phys. Rev. Lett.* **33**, 820 (1974).

²S. M. Shapiro, R. J. Birgeneau, and E. Bucher, *Phys. Rev. Lett.* **34**, 470 (1975).

³M. H. Dickens, C. G. Shull, W. C. Koehler, and R. M. Moon, *Phys. Rev. Lett.* **35**, 595 (1975).

⁴N. Kroo and Z. Szentirmay, *Phys. Rev. B* **10**, 278 (1974).

⁵G. Bauer and E. Seitz, *Solid State Commun.* **11**, 179 (1972).

⁶J. B. Boyce and C. P. Slichter, *Phys. Rev. B* **13**, 379 (1976).

⁷H. Alloul, *Phys. Rev. Lett.* **35**, 460 (1975).

⁸P. Steiner, S. Hufner, and W. V. Zdrojewski, *Phys. Rev. B* **10**, 4704 (1974).

⁹G. E. Gurgenshvili, A. A. Neresyan, and G. A. Kharadze, *Zh. Eksp. Teor. Fiz.* **56**, 2028 (1969) [*Sov. Phys. JETP* **29**, 1089 (1969)].

¹⁰K. A. Gschneidner, Jr., R. O. Elliott, and R. R. McDonald, *J. Phys. Chem. Solids* **23**, 555, 1191, 1201 (1962).

¹¹J. M. Lawrence, M. C. Croft, and R. D. Parks, *Phys. Rev. Lett.* **35**, 289 (1975).

¹²The data above 100°K were taken from K. H. Mader and W. M. Swift, *J. Phys. Chem. Solids* **29**, 1759 (1968).

¹³A. S. Edelstein, T. O. Brun, G. H. Lander, O. D. McMasters, and K. A. Gschneidner, Jr., in *Magnetism and Magnetic Materials-1974*, AIP Conference Proceedings No. 24, edited by C. D. Graham, Jr., G. H. Lander, and J. J. Rhyne (American Institute of Physics, New York, 1975), p. 428.

¹⁴G. H. Lander and T. O. Brun, *J. Chem. Phys.* **53**, 1387 (1970); M. Blume, A. J. Freeman, and R. E. Watson, *J. Chem. Phys.* **37**, 1245 (1962).

¹⁵K. H. Mader and W. M. Swift, *J. Phys. Chem. Solids* **29**, 1759 (1968).

¹⁶The CF splitting in γ -Ce is 67 K. See A. H. Millhouse and A. Furrer, *Solid State Commun.* **15**, 1303 (1974).

Observation of Two-Dimensional Phases Associated with Defect States on the Surface of TiO_2 †

Victor E. Henrich, G. Dresselhaus, and H. J. Zeiger

Lincoln Laboratory, Massachusetts Institute of Technology, Lexington, Massachusetts 02173

(Received 12 April 1976)

Surface electronic states associated with defects produced by Ar-ion bombardment of TiO_2 crystals have been studied by ultraviolet-photoemission, electron-energy-loss, and Auger spectroscopy and low-energy-electron diffraction. Evidence is given for three distinct phases dependent upon the extrinsic surface-defect concentration. Phase I contains isolated surface states 0.7 eV below the conduction band, phase II is associated with the creation of Ti^{3+} pairs, and phase III consists of a surface layer of ordered Ti_2O_3 .

The importance of transition-metal oxides in a wide range of catalytic and electrocatalytic applications has spurred a great deal of research on their surface properties and on the role of

surface defects in their catalytic activity. For example, surface states on TiO_2 have recently been shown to play a central role in the TiO_2 -catalyzed photoelectrolysis of water.¹ Previous

studies of surface defects and adsorbed molecules on transition-metal oxides by such techniques as electron-spin resonance² and infrared absorption³ have recently been augmented by investigations of single-crystal surfaces using relatively new theoretical and experimental techniques such as cluster calculations⁴ and various electron spectroscopies.⁵ We have previously reported⁶ electron-energy-loss spectra (ELS) of TiO_2 , Ti_2O_3 , and $\text{TiO}_{0.87}$ that showed the existence of surface states on TiO_2 associated with surface Ti^{3+} ions.

In this Letter we present the results of a combined ultraviolet-photoemission-spectroscopy (UPS), ELS, low-energy-electron-diffraction (LEED), and Auger study of defect states on the surface of TiO_2 (rutile) as the defect density is varied by Ar-ion bombardment. From these results we infer the existence of three different surface-defect phases. At low defect densities, Ar-ion bombardment produces extrinsic surface states about 0.7 eV below the TiO_2 conduction-band edge which are associated with disorder-induced Ti^{3+} -oxygen-vacancy complexes. As the concentration of defects is increased, a pairing of Ti^{3+} ions similar to that in Ti_2O_3 occurs. Still further bombardment produces ordering of the Ti^{3+} ion pairs into a Ti_2O_3 -like surface structure. These extrinsic surface states are distinct from the intrinsic gap states to be expected on the surface of TiO_2 due to the truncation of the crystal potential.⁴

All electron spectra were measured with a double-pass cylindrical-mirror spectrometer. Auger and ELS spectra were excited by an electron beam coaxial with the spectrometer, while UPS spectra were excited with the He I line (21.2 eV) from a microwave discharge lamp. Most of the ELS data were taken with a primary energy of 100 eV at normal incidence.

The surface investigated was a (110) face of a TiO_2 single crystal which was polished and etched, then cleaned by Ar-ion sputter etching and annealed at about 1100 K by electron bombardment in the ultrahigh-vacuum system. After annealing, the sample was deep blue, indicating that roughly 10^{19} oxygen vacancies per cm^3 had been produced.⁷ The annealed surface exhibited excellent (110) LEED patterns, and no impurities were detected by Auger spectroscopy. To produce surface defects, the sample was then bombarded with 500-eV Ar ions incident at about 20° to the surface plane.

Figure 1(a) shows the UPS spectrum [photoelec-

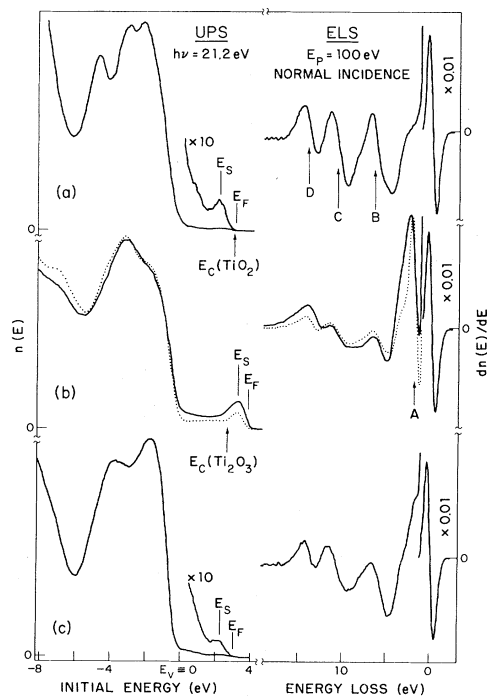


FIG. 1. UPS and ELS spectra for (a) annealed TiO_2 (110), (b) Ar-ion-bombarded TiO_2 (110) (solid curves) and vacuum-fractured Ti_2O_3 (dotted curves), and (c) Ar-ion-bombarded TiO_2 (110) after exposure to 10^8 L of oxygen. For UPS, zero of the initial-state energy is the upper edge of the valence band.

tron distribution $n(E)$ versus initial energy E of emitted electrons] and the ELS spectrum [derivative $dn(E)/dE$ of the secondary-electron distribution versus energy loss E] for the annealed TiO_2 (110) surface. The UPS spectrum contains a weak peak, with its maximum at an energy E_s about 2.3 eV above the upper edge of the valence band E_v ; this peak is due to excitation of electrons from states lying in the bulk band gap of TiO_2 , which is 3.05 eV.⁷ These are extrinsic surface states associated with a small density of residual surface defects, since no such peak is observed for vacuum-fractured⁸ surfaces of either reduced or unreduced TiO_2 . The Fermi level E_F lies near the bottom edge of the bulk conduction band E_c . The structure in the ELS spectrum of Fig. 1(a) reflects only three peaks in $n(E)$, labeled B, C, and D, that are common to all of the surfaces studied here and arise from oxygen-to-Ti cross excitations.⁶

Figure 1(b) shows the spectra obtained after several minutes of Ar-ion bombardment. In the UPS spectrum, the surface-state peak is 50–100 times more intense than on the annealed surface,

E_s has shifted to 3.2 eV above E_v , E_F has risen to 3.9 eV, and the structure at $E < 0$ associated with the valence band has also changed. The ELS spectrum now exhibits a strong peak (A) at about 1.9 eV that is associated with d -to- d transitions involving Ti^{3+} ions.⁶ Both spectra are remarkably similar to those of vacuum-fractured Ti_2O_3 , which are shown by the dotted curves in Fig. 1(b). However, the primary-electron-energy dependence of the ELS spectra⁹ shows that ELS peak A is entirely of surface origin in bombarded TiO_2 but partly of bulk origin in Ti_2O_3 .

When the TiO_2 surface of Fig. 1(b) was exposed to 10^8 L (1 L = 10^{-6} Torr sec) of oxygen, the spectra of Fig. 1(c) were obtained. The intensity of the UPS surface-state peak has been greatly reduced, E_s has shifted back to 2.5 eV, and additional changes have occurred in the valence-band structure. The ELS peak A is much weaker but has not completely disappeared.

Figure 2 shows the results of experiments in which an annealed TiO_2 surface was subjected first to a series of Ar-ion bombardments (solid points) and then to a series of oxygen exposures

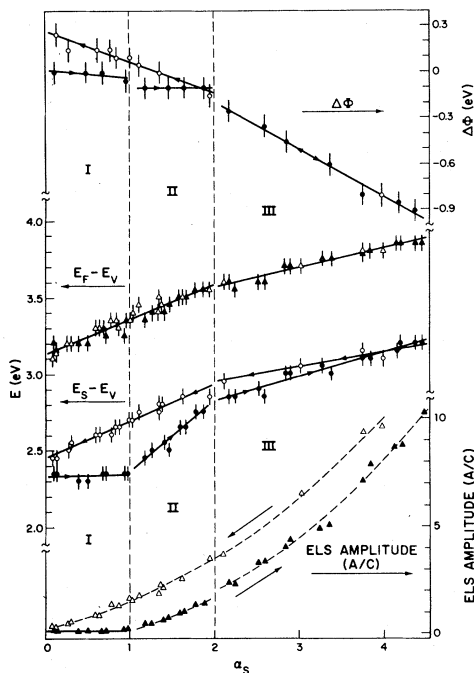


FIG. 2. Work function change ($\Delta\Phi$), Fermi level ($E_F - E_v$), position of surface-state UPS peak ($E_s - E_v$), and normalized amplitude of ELS peak A versus normalized intensity of UPS surface-state peak (α_s) for Ar-ion bombardment (solid points) and subsequent oxygen exposure (open points) of TiO_2 (110) surface. Arrows indicate sequence in which data were taken.

(open points). The abscissa parameter α_s , which is a rough measure of the number of occupied surface states, is the integrated intensity of the UPS surface-state peak (with a linear background subtracted) normalized to its value at the boundary between regions I and II in Fig. 2 (see below). The value of α_s is lowest for the annealed surface; it is increased by Ar-ion bombardment and decreased by oxygen exposure. Four quantities are plotted against α_s : (1) $\Delta\Phi$, the difference between the work functions (determined from the UPS spectra) of the treated surface and the annealed surface; (2) $E_F - E_v$; (3) $E_s - E_v$; and (4) the amplitude of ELS peak A, normalized to that of ELS peak C (see Fig. 1). The last three quantities were very reproducible, and data from two independent runs are plotted in Fig. 2. The data obtained on initial Ar-ion bombardment fall into three regions as a function of α_s . (The solid lines shown in Fig. 2 represent least-squares linear fits to the data within either one or two of the regions, while the dashed lines are merely smooth curves.) We associate these three regions, designated as I, II, and III, with three different surface phases.

In region I ($\alpha_s < 1$), the intensity of the UPS peak due to the extrinsic surface state increases by more than a factor of 10, but the peak remains 2.3 eV above E_v . The ELS spectra in this region change very little, with no indication of peak A. This shows that the extrinsic state has no well-defined excited state with an energy greater than about 1.2 eV (excited states closer than 1.2 eV to the intense elastic peak could not have been resolved). By $\alpha_s = 1$ the excellent LEED patterns of the annealed surface have virtually disappeared, but the Auger spectra show almost no loss of oxygen. Thus within region I the atomic arrangement of the surface becomes disordered without appreciable change in surface stoichiometry. Region II ($1 < \alpha_s < 2$) is characterized by the appearance of the sharp ELS peak A, the shifting of the UPS surface-state peak away from the valence band, and a loss of oxygen from the surface. These results indicate that a different type of extrinsic surface state, associated with surface reduction, is being created in region II; it has a ground-state energy higher than that of the state in region I and a well-defined excited state. Region III ($\alpha_s > 2$) is defined by a decrease in the slope of $E_s - E_v$ versus α_s by a factor of 3 and by a sharp decrease in $\Delta\Phi$. The position and amplitude of ELS peak A vary smoothly through regions II and III, and only a small change in the

slope of $E_F - E_v$ versus α_s is seen at $\alpha_s = 2$.

When the heavily reduced, disordered TiO_2 surface $\alpha_s > 4$ is exposed to oxygen at room temperature, $E_F - E_v$ is reversible and E_s remains 0.7 eV below E_F over the entire range of α_s . All four measured quantities vary smoothly for $\alpha_s < 2$. Sufficient exposure to oxygen reduces α_s almost to zero. If the surface is then bombarded with Ar ions, α_s is again increased, and the data essentially reproduce the curves obtained during oxygen exposure.

The constant value of $E_s - E_v$ in region I indicates that the surface defects created are non-interacting. The data do not permit a determination of the exact nature of these defects, however. One likely possibility is a vacancy resulting from the displacement of an oxygen ion from a Ti-Ti bridge site to another site, perhaps to a position over one of the fivefold-coordinated surface Ti ions. This vacancy has an attractive Madelung potential and is capable of trapping an electron to form a Ti^{3+} -oxygen-vacancy complex. The ground-state energy of this complex would be below the bulk-conduction-band edge in TiO_2 , consistent with the observed value of $E_s - E_v$.

The discontinuities observed at $\alpha_s = 1$ indicate the occurrence of a surface phase transition which we interpret as the beginning of strong interaction between surface Ti^{3+} ions. At this point the sample has been hit by an average of one Ar ion per surface unit cell, as determined from measured ion-beam parameters. The appearance of peak A in the ELS spectrum and the rise of $E_s - E_v$ toward its value in Ti_2O_3 are strong evidence for the formation of pairs of Ti^{3+} ions that share a common oxygen octahedral face.¹⁰ The bonding and antibonding states derived from the $3d$ orbitals of such Ti^{3+} pairs constitute the conduction bands in Ti_2O_3 ,¹⁰ and we believe that ELS peak A is due to a transition between such pair states. We attribute the onset of pairing at $\alpha_s = 1$ to the Madelung destabilization of the TiO_2 surface structure due to the presence of a high density of surface Ti^{3+} and O^- ions.¹¹ The surface is then stabilized by a loss of oxygen and the displacement of some of the Ti^{3+} ions into empty octahedral sites that exist 1.6 Å below the unreconstructed TiO_2 (110) surface, forming Ti_2O_3 -like Ti^{3+} pairs.

As the density of Ti^{3+} pairs increases, a cooperative phase transition associated with the ordering of the pairs occurs at $\alpha_s = 2$. In effect, small areas of Ti_2O_3 begin to form on the surface, causing the average work function to decrease

toward the lower values that we have observed for vacuum-fractured Ti_2O_3 . The value of $E_s - E_v$ continues to rise in region III as more Ti^{3+} pairs are created at the expense of the defects present in region I. After long Ar-ion bombardment times, α_s reaches a constant value of 4 to 5. At this point the UPS and ELS spectra are almost indistinguishable from those of Ti_2O_3 [see Fig. 1(b)], confirming the similarity of the two surface structures. Furthermore, vacuum-fractured single-crystal Ti_2O_3 follows oxidation curves similar to those for heavily ion-bombarded TiO_2 , providing additional evidence for this similarity.

The type of investigation reported here offers the possibility of bridging the gap between ideal and real surfaces by studying the electronic states of surface defects as a continuous function of defect concentration. The interaction of these defect states with ambient gases, such as the oxygen used here, can be studied as a step toward understanding the catalytic behavior of real surfaces. Recent experiments on the photoelectrolysis of water in cells with heavily reduced TiO_2 oxygen electrodes¹ indicate that the photoelectrolytic activity of the electrodes is correlated with the presence of filled surface states located about 1 eV below E_c . These states lie close in energy to the defect surface states reported in this Letter, and we are currently examining the relationship between them.

The authors acknowledge helpful discussions with J. B. Goodenough, J. G. Mavroides, and A. O. E. Animalu, and the technical assistance of B. Feldman.

† This work was sponsored by the Department of the Air Force.

¹J. G. Mavroides, D. I. Tchernev, J. A. Kafalas, and D. F. Kolesar, *Mater. Res. Bull.* **10**, 1023 (1975); J. G. Mavroides, private communication.

²C. Naccache, P. Meriaudeau, M. Che, and A. J. Tench, *Trans. Faraday Soc.* **67**, 506 (1971).

³P. Jackson and G. D. Parfitt, *Trans. Faraday Soc.* **67**, 2469 (1971).

⁴F. J. Morin and T. Wolfram, *Phys. Rev. Lett.* **30**, 1214 (1973); T. Wolfram, in "Electrocatalysis on Non-Metallic Surfaces," National Bureau of Standards Special Publication (U.S. GPO, Washington, D. C., to be published).

⁵R. A. Powell and W. E. Spicer, *Phys. Rev. B* **13**, 2601 (1976).

⁶V. E. Henrich, H. J. Zeiger, and G. Dresselhaus, in "Electrocatalysis on Non-Metallic Surfaces," National Bureau of Standards Special Publication (U.S. GPO, Washington, D.C., to be published).

⁷D. C. Cronmeyer, Phys. Rev. **87**, 876 (1952).

⁸We use the term fractured because TiO_2 and Ti_2O_3 do not cleave well. The surfaces obtained were rough and exhibit poor LEED patterns.

⁹V. E. Henrich, G. Dresselhaus, and H. J. Zeiger,

Phys. Rev. Lett. **36**, 158 (1976).

¹⁰J. B. Goodenough, Prog. Solid State Chem. **5**, 145 (1972).

¹¹G. Dresselhaus, H. J. Zeiger, and V. E. Henrich, Bull. Am. Phys. Soc. **21**, 321 (1976).

Adsorbate-Level Splitting in Hydrogen Chemisorption

B. Feuerbacher and R. F. Willis

Surface Physics Group, Astronomy Division, European Space Research and Technology Centre, Noordwijk, Holland

(Received 29 December 1975)

The electronic energy levels of a hydrogen (1×1) monolayer adsorbed on the (100) tungsten single-crystal face have been investigated by angle-resolved photoemission. *Three* bands of adsorbate levels are found that disperse and split with angle, at energies of about 2, 6, and 12 eV below the Fermi level. The results suggest that hydrogen chemisorption takes place by interaction with localized directional surface-group orbitals of the tungsten *d* band.

The adsorption of hydrogen on the (100) surface of tungsten can be regarded as a system that models the bonding of a simple *1s* adsorbate to a tight-binding *d*-band substrate. As such it has received considerable theoretical attention,¹⁻⁷ particularly as regards the extent to which a localized-orbital approach provides a viable model. Distinct practical advantages of the hydrogen-tungsten system have stimulated a large amount of experimental work using surface-sensitive techniques such as thermal desorption,⁸ low-energy electron diffraction (LEED),⁹ electron-stimulated desorption,¹⁰ and field-emission¹¹ or photoemission spectroscopy.¹²⁻¹⁴ This Letter describes results of a complete series of angle-resolved photoemission studies on adsorbate-induced resonance levels of a hydrogen monolayer (full coverage) on a W(100) surface. *Three* bands of adsorbate-resonance features are found at energies around 2, 6, and 12 eV below the Fermi level, which disperse and split with polar angle. The relatively narrow width of the adsorbate-induced photoemission spectral features, and their apparent grouping in the angular distribution, is interpreted as being indicative of chemisorption bonds involving only selective groups of substrate *d* orbitals,^{2,5} leading to localized, directional bonding within a surface molecular complex.¹⁵

The experiments have been performed in an ultrahigh-vacuum system with a base pressure below 1×10^{-10} Torr. The cleaned crystal was placed in the center of a metallic sphere¹⁶ that ensured an electrostatic and magnetically shielded "field-free" region. Light was incident at 45°

to the crystal surface, and a slot along the periphery of the sphere allowed the emitted photoelectrons to enter a 127° electrostatic deflection analyzer with 0.2-eV energy resolution, sampling a $2^\circ \times 2^\circ$ solid angle. Polar scans were possible for all azimuth directions, but the results presented here are restricted to the principal $\langle 10 \rangle$ and $\langle 11 \rangle$ azimuths. Measurements were performed on saturation-coverage (1×1) hydrogen monolayers to avoid complications due to adsorbate-induced surface-umklapp processes that occur at submonolayer coverages.¹⁴ The light source was an open helium resonance lamp, which caused the pressure in the system to rise during operation to 1×10^{-8} Torr due to He gas. The present data were taken after initial saturation coverage had been obtained with a background hydrogen pressure of 1×10^{-7} Torr in the chamber. The results were later cross checked against data obtained in a closed vacuum system of better than 1×10^{-10} Torr at 10.2-eV excitation energy, to ensure that the stream of neutral He atoms from the light source did not cause changes in the observed adsorbate system.

Measurements of photoelectron energy distribution spectra were recorded for clean and hydrogen-covered surfaces consecutively in 5° polar-angle steps along the two principal azimuth directions $\langle 10 \rangle$ and $\langle 11 \rangle$. Typical results are shown in Fig. 1 for normal emission ($\theta = 0^\circ$), 30° , and 60° polar angle along the $\langle 10 \rangle$ azimuth. The spectra for normal emission agree with previously published results.^{12,17} A prominent peak of twice the intensity of the substrate emission is found in the